The Reproducibility of Phospholipid Analyses by MALDI-MSMS

Catherine J. Pridmore,[a] Matthew R. Hicks,[b] Jackie A. Mosely*[a] and John M. Sanderson*[a]

The identification of phosphocholine and phosphoethanolamine lipids by MALDI TOF/TOF, including characterisation of the headgroup and delineation of the acyl chain at each position of the glycerol backbone, has been explored using lipids representative of each type. The relative intensities of fragments involving the neutral loss of one or other of the acyl chains of 1-palmitoyl-
10 2-oleoyl-sn-glycero-3-phosphoethanolamine (POPE), 1-palmitoyl-2-oleoyl-sn-glycero-3-phosphocholine (POPC) and 1-oleoyl-2-palmitoyl-sn-glycero-3-phosphocholine (OPPC) were compared. For POPC and POPE, a statistical preference for the loss of the chain from the sn-1 position was observed in the presence of lithium. For OPPC this selectivity was reversed for one of the fragments. In the absence of lithium, fragmentation was favoured at the sn-2 position for all
15 lipids. In all cases, spectra obtained in the presence of lithium yielded more intense product ion peaks. Although Collision Induced Dissociation (CID) could be used for complete lipid characterisation, LIFT™ was found to be a better method due to the presence of a greater number of distinguishing product ion peaks and a better shot-to-shot reproducibility of peak intensities.

Introduction

20 Glycerophospholipids are the most abundant type of lipid found in cell membranes. The characteristics of membranes from different types of cell are defined by the chemical identities of their constituent phospholipids. Factors such as headgroup charge, degree of unsaturation and acyl chain
25 length influence the fundamental physical parameters of the membrane, such as bilayer thickness, phase-transition temperature and mixing behaviour.[1] All of these factors highlight the importance of being able to identify fully phospholipids, including the chemical identity of both acyl
30 chains and the nature of the headgroup. Mass spectrometry has the potential to fulfil this need through the identification of suitable fragments corresponding to each of these key functional groups.

Matrix-assisted laser desorption/ionisation-time of flight
35 mass spectrometry (MALDI-TOF MS) analysis of lipids has been conducted using both commonly-used matrices such as isomers of 2,5-dihydroxybenzoic and 2,4,6-trihydroxyacetophenone,[2,3] as well as more novel species such as ionic liquids.[4] The identification of product ion peaks
40 following fragmentation of lipids by MSMS in the presence of metal cations is a good method for lipid analysis. Upon fragmentation of both $[M + H]^+$ and $[M + Na]^+$ for a number of phosphocholine (PC) lipids by post-source decay (PSD) MALDI-TOF MSMS, the $[M + H]^+$ product ion spectra
45 showed only one strong product ion peak, corresponding to the headgroup at m/z 184, while the $[M + Na]^+$ product ion spectra showed a number of peaks, including those corresponding to the loss of one or other of the acyl chains.[5] Similar studies have been carried out on the effect of adding
50 lithium salts. Stübiger and Belgacem studied lipids from several classes,[3] including glycerophospholipids, comparing the MALDI-MSMS product ion spectra of $[M + Na]^+$, $[M +$

$Li]^+$ and $[M + H]^+$. The $[M + Li]^+$ product ion spectra were found to give more intense product ion peaks than those of $[M
55 + Na]^+$ and include the appearance of protonated and lithium containing product ions separated by 6 Da. Both of these observations are advantageous for lipid identification and have been put to good use for techniques such as MALDI imaging.[6]
60 In order to identify fully a phospholipid, it is necessary to identify the acyl chain at each position of the glycerol backbone, termed the sn-1 and sn-2 positions (Fig. 1). The relative intensities of peaks corresponding to the loss of the chains from the sn-1 and sn-2 positions in tandem mass
65 spectra are a potential method of determining this, although published data for PC and phospoethanolamine (PE) lipids in the presence and absence of sodium and lithium salts reveal a number of inconsistencies. This is manifested both in terms of the ability to observe peaks corresponding to the loss of both
70 of the acyl chains, and in their relative intensities if they are observed.[3,5-25] Evidence for the loss of the acyl chains from each of the sn-1 and sn-2 positions was reported in all cases where fragmentation was carried out using collision induced dissociation (CID) in either a sector instrument,[8,9,18,20,24,25] a
75 linear ion trap,[14,16] or a MALDI-TOF/TOF.[3,6,15] In approximately 50% of cases involving fragmentation by Post Source Decay (PSD) or seamless Post Source Decay (sPSD),[5,8,17] it was reported that fragments corresponding to the release of the acyl chains were not present.[8,17] When
80 fragmentation occurred by CID in a triple quadrupole a range of outcomes resulted. These included: no evidence for cleavage of the acyl chains;[11] evidence of the loss of the acyl chain from each position with a statistical difference in their intensities;[10,11,13,22] evidence of the loss of the acyl chain from
85 each position with no statistical difference in their intensities;[19] and evidence of the loss of each chain as different types of fragments, with differences in the relative

intensities of losses from the *sn*-1 and *sn*-2 positions depending on fragment type.[12] A clear example of the range of outcomes is presented by $[PC + Na]^+$, where a lack of observable fragments corresponding to the loss of the acyl chains was reported when this ion underwent sPSD.[8] Al-Saad *et al.* and Landgraf *et al.* have reported the appearance of fragments corresponding to loss of the acyl chains from both the *sn*-1 and *sn*-2 positions, with a higher intensity of the peaks corresponding to the loss of the chain from the *sn*-1 position when fragmenting $[PC + Na]^+$ by PSD or by CID in a linear ion trap.[5,16] Kim *et al.* fragmented the same ion by high energy CID in a sector instrument and reported the direct opposite, with a higher intensity of the peaks corresponding to the loss of the acyl chain from the *sn*-2 positions.[20] These data highlight the need for a systematic study of the effects of different MSMS methods on the relative cleavage of the acyl chains.

The work reported herein describes a systematic study by MALDI-TOF/TOF of two phosphocholines and a phosphoethanolamine using LIFT™ technology in the absence of a collision gas,[26] and using Collision Induced Dissociation (CID) in the presence of argon. The benefits of the addition of a lithium salt during the MALDI TOF/TOF analysis of lipids are reported, along with the relative intensities of the product ions corresponding to the loss of the acyl chains from the *sn*-1 and *sn*-2 positions of the lithiated and protonated molecular ions, determined from a number of automated analyses.

Experimental

Reagents

1-palmitoyl-2-oleoyl-*sn*-glycero-3-phosphoethanolamine (POPE), and 1-oleoyl-2-palmitoyl-*sn*-glycero-3-phosphocholine (OPPC) were purchased from Avanti Polar Lipids (Alabama, USA). 1-palmitoyl-2-oleoyl-*sn*-glycero-3-phosphocholine (POPC), 2,5-dihydroxybenzoic acid (DHB), lithium chloride, poly(ethylene glycol) 600 and ethanol (HPLC grade) were purchased from Sigma-Aldrich, UK. Chloroform (reagent-grade) was purchased from Fisher Scientific UK. Water with resistivity >18 MΩ/cm was purified using a Milli-Q Direct Q system from Millipore (Millipore (UK) Ltd.).

Sample preparation

The matrix, DHB, was prepared at a concentration of 30 mg/ml in EtOH/H$_2$O (50 % v/v) for analyses in the absence of lithium. For experiments in the presence of lithium, DHB was prepared at a concentration of 30 mg/mL in solutions of 5 mM to 100 mM LiCl in EtOH/H$_2$O (50 % v/v) (a concentration of 100 mM LiCl was used unless otherwise stated). These solutions were mixed at a ratio of 9:1 v/v with lipid solutions (each 1 mg/mL in CHCl$_3$). For manual experiments, 1 μL of the matrix/lipid solution was spotted onto the target and allowed to air dry. For automated runs, 2 × 0.5 μL aliquots were spotted on top of each other and allowed to dry between applications.

Mass spectrometry

MS and MSMS experiments were carried out using an Autoflex II MALDI-TOF/TOF spectrometer with a 337 nm nitrogen laser (Bruker Daltonics Ltd., Coventry, UK). This was calibrated for MS experiments with the sodium adducts of poly(ethylene glycol) 600. A ground steel target plate was cleaned with methanol and acetone prior to use. Positive ion MS experiments were conducted using the reflectron for enhanced performance. Positive ion MSMS experiments were conducted using the LIFT capability in the absence of a collision gas at a source pressure of approximately 2.5×10^{-7} mBar unless otherwise stated. For CID experiments, argon was used a collision gas at a source pressure of approximately 8.5×10^{-7} mBar. Isolation of the protonated ion was sufficient with instrument defaults. The isolation windows for LIFT of the lithium adduct ions were set in order to exclude the $[POPC + H]^+$ ion from fragmentation of $[POPC + Li]^+$, and both $[POPE + H]^+$ and $[POPE - H + 2Li]^+$ from the fragmentation of $[POPE + Li]^+$. For the automated LIFT analysis of $[POPE + Li]^+$ the figures represent the narrowest window from which results could successfully be produced. For CID the precursor ion isolation window could not be altered from the default setting of ± 1 % due to software constraints. A summary of the isolation windows for all precursor ions is given in Table S1 (ESI). Lithium exists as two isotopes, ^6Li and ^7Li, with isotopic abundances of 7.5 and 92.5 respectively.[27] It was not possible to separate the isotopes when selecting $[M + Li]^+$ precursor ions, but the ^7Li adduct is referred to in all discussion of fragments. Data were analysed using Flex Analysis version from 3.0 Bruker Daltonics Ltd (Coventry, UK).

Results and Discussion

MALDI-MS analysis

The lipids POPE (Fig. 1a) and POPC (Fig. 1b) were studied by MALDI-MS. The appearance in the mass spectra of these lipids of peaks separated by 6 Da (corresponding to $[M + H]^+$ and $[M + ^7Li]^+$ in the case of POPC; $[M + H]^+$, $[M + ^7Li]^+$ and $[M - H + 2\,^7Li]^+$ in the case of POPE) provided a visual aid for the identification of lipid molecular ions, as exemplified in the in the spectra of POPE (ESI, Fig. S1) and POPC (ESI, Fig. S2). For POPE, $[M + H]^+$ was observed at the lowest intensity, with $[M - H + 2\,^7Li]^+$ and $[M + ^7Li]^+$ observed at progressively higher intensities. $[M + ^6Li]^+$ and $[M - H + ^6Li + ^7Li]^+$ were present as minor peaks. In the case of POPC, $[M + H]^+$ and $[M + ^7Li]^+$ were observed as major peaks with $[M + ^6Li]^+$ as a minor peak. The additional doubly lithiated peaks observed in spectra of POPE are accounted for by the ability of the ethanolamine ammonium group (pKa=9.8) to exist in a neutral form (unattainable with the choline 4° ammonium group). The full scan mass spectra showed evidence that the lipids fragment readily (ESI, Fig. S3).

Direct comparison with matrix-only spectra showed *m/z* values corresponding to the headgroup in the spectra of $[POPC + H]^+$ and $[POPC + Li]^+$, and to $[POPE - OP(O)_2O(CH_2)_2NH_3]^+$ in the spectra of $[POPE + H]^+$ and $[POPE + Li]^+$.
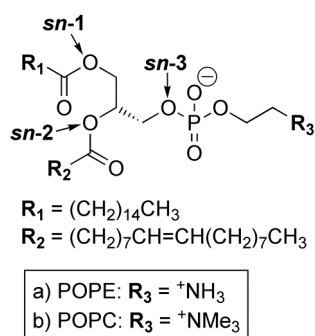
Fig. 1 The structures of a) POPE and b) POPC. The *sn*-1, *sn*-2 and *sn*-3 positions on the glycerol backbone of POPE are labelled, along with sections of the acyl chains which are referred to as R_1 and R_2 in the main text.

No evidence for the acyl chains themselves, or for their loss, was observed in any of the four spectra.

MALDI-MSMS analysis

POPE molecular ions. MALDI-MSMS spectra of both [POPE + H]$^+$ and [POPE + Li]$^+$ showed evidence of [POPE − OP(O)$_2$O(CH$_2$)$_2$NH$_3$]$^+$, corresponding to loss of a headgroup fragment, as the dominant species (Fig. 2).
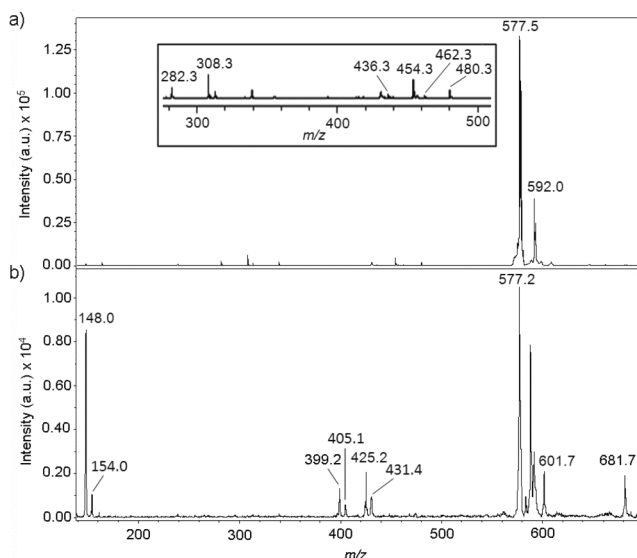

Fig. 2 MALDI-MSMS spectra of (a) [POPE + H]$^+$ and (b) [POPE + Li]$^+$.

The product ion spectra of both [POPE + H]$^+$ and [POPE + Li]$^+$ exhibited peaks that could be assigned to either fragments of both acyl chains or the headgroup, or products arising from their neutral loss. The product ion spectrum of [POPE + H]$^+$ (Fig. 2a, Table 1) showed two pairs of peaks corresponding to the loss of the acyl chains from the *sn*-1 and *sn*-2 positions as different types of fragments. The spectrum of [POPE + Li]$^+$ (Fig. 2b, Table 1) only contained one pair of peaks from which both acyl chains could be identified. These peaks, corresponding to [POPE − R$_2$COO − (CH$_2$)$_2$NH$_3$ + H + ^{7}Li]$^+$ and [POPE − R$_1$COO − (CH$_2$)$_2$NH$_3$ + H + ^{7}Li]$^+$, had much greater intensities relative to the peak corresponding to [POPE − OP(O)$_2$O(CH$_2$)$_2$NH$_3$]$^+$, than any of the peaks corresponding to the loss of an acyl chain observed in the spectrum of [POPE + H]$^+$.

Table 1 Product ions observed in MALDI-MSMS spectra of [POPE + H]$^+$ and [POPE + Li]$^+$.

[POPE + H]$^+$		[POPE + Li]$^+$	
m/z	Product ion^{a,b}	*m/z*	Product ion^{a,b}
282.3	[R$_2$COOH]$^+$	148.0	[OP(O)$_2$OEtn + ^{7}Li + H]$^+$
308.3	[R$_2$COOCH$_2$CH$_2$]$^+$	399.2	[M - R$_2$COO − Etn + H + ^{7}Li]$^+$
436.3	[M - R$_2$COO]$^+$	425.2	[M - R$_1$COO − Etn + H + ^{7}Li]$^+$
454.3	[M - R$_2$CO + 2H]$^+$	577.2	[M - OP(O)$_2$OEtn]$^+$
462.3	[M − R$_1$COO]$^+$	601.7	[M - P(O)$_2$OEtn + H + ^{7}Li]$^+$
480.3	[M - R$_1$CO + 2H]$^+$	681.7	[M − Etn + 2H + ^{7}Li]$^+$
577.5	[M - OP(O)$_2$OEtn]$^+$		
592.0	[M - P(O)$_2$OEtn - 2H]$^+$		

^{a} R$_1$ and R$_2$ are defined in Fig. 1.

^{b} Etn = (CH$_2$)$_2$NH$_3$

As a consequence, the product ion spectra of the lithium adducts of POPC were clearer and allowed easier identification of the lipid. Less intense peaks could be observed in the [POPE + Li]$^+$ product ion spectrum at *m/z* 405 and *m/z* 431 (Fig. 2b). These are assigned to [POPE − R$_2$COO − 2H + 2^{7}Li]$^+$ and [POPE − R$_1$COO − 2H + 2^{7}Li]$^+$ respectively and have arisen from incomplete isolation of the [POPE + Li]$^+$ parent, with an isolation window of ± 5 Da, allowing some dissociation products from [POPE − H + 2Li]$^+$ to be observed.

POPC molecular ions. The product ion spectra of both [POPC + H]$^+$ and [POPC + Li]$^+$ had a peak identified as [OP(O)$_2$(CH$_2$)$_2$NMe$_3$ + 2H]$^+$, corresponding to a headgroup fragment, as the dominant species (Fig. 3).
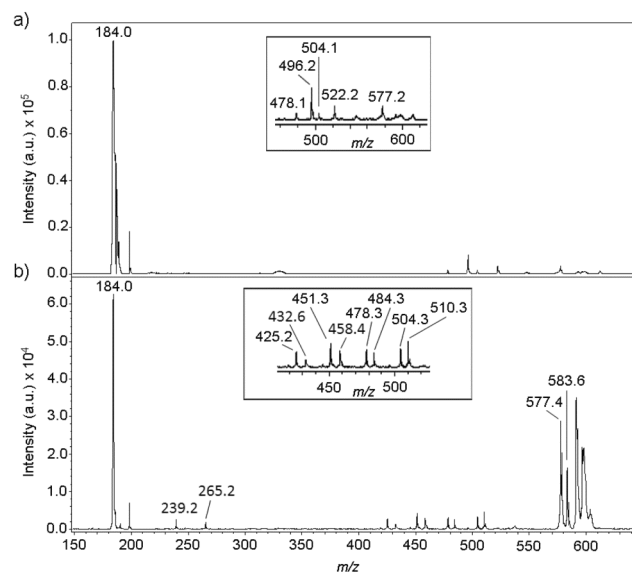

Fig. 3 MALDI-MSMS spectra of [POPC + H]$^+$ (a) and [POPC + Li]$^+$ (b).

Both spectra, however, contained other fragments that permitted identification of each of the acyl chains. The product ion spectrum of [POPC + H]$^+$ (Fig. 3a, Table 2) showed two pairs of peaks corresponding to the loss of the acyl chains, while the spectrum of [POPC + Li]$^+$ (Fig. 3b, Table 2) showed four pairs of peaks from which the acyl chains could be identified.

Table 2 Product ions observed in MALDI-MSMS spectra of [POPC + H]+ and [POPC + Li]+.

	[POPC + H]$^+$		[POPC + Li]$^+$
m/z	Product ion^{a,b}	*m/z*	Product ion^{a,b}
184.0	[OP(O)$_2$Chn + 2H]$^+$	184.0	[OP(O)$_2$Chn + 2H]$^+$
478.1	[M - R$_2$COO]$^+$	239.2	[R$_1$CO]$^+$
496.2	[M - R$_2$CO + 2H]$^+$	265.2	[R$_2$CO]$^+$
504.1	[M - R$_1$COO]$^+$	425.2	[M - R$_2$COO - NMe$_3$ – H + ^{7}Li]$^+$
522.2	[M - R$_1$CO + 2H]$^+$	451.3	[M - R$_1$COO - NMe$_3$ – H + ^{7}Li]$^+$
577.2	[M - OP(O)$_2$Chn]$^+$	478.3	[M - R$_2$COO]$^+$
		484.3	[M - R$_2$COO – H + ^{7}Li]$^+$
		504.3	[M - R$_1$COO]$^+$
		510.3	[M - R$_1$COO – H + ^{7}Li]$^+$
		577.4	[M - OP(O)$_2$Chn]$^+$
		583.6	[M - OP(O)$_2$Chn – H + ^{7}Li]$^+$

^{a} R$_1$ and R$_2$ are defined in Fig. 1.

^{b} Chn = (CH$_2$)$_2$NMe$_3$

5   Most of the peaks corresponding to the neutral loss of the acyl chains in the product ion spectrum of [POPC + Li]$^+$ had a greater intensity relative to the predominant headgroup peak ([OP(O)$_2$(CH$_2$)$_2$NMe$_3$ + 2H]$^+$) than the peaks resulting from neutral loss of the acyl chains in the spectrum of [POPC +
10 H]$^+$. This higher relative intensity for products of lithium adduct fragmentation should be useful in cases where sensitivity is an issue. Peaks can also be observed at *m/z* 432 and *m/z* 458 in the [POPC + Li]$^+$ product ion spectrum (Fig. 3b), which due to their peak shape are assigned as metastable
15 products.

As with the molecular ions in the MS spectra of both lipids, characteristic peaks in the product ion spectrum of [POPC + Li]$^+$ (Fig. 3b) occurred as pairs of protonated and lithium adduct ions separated by 6 Da. These are exemplified by pairs
20 of peaks at *m/z* 478 and *m/z* 484, corresponding respectively to [POPC - R$_2$COO]$^+$ and [POPC - R$_2$COO – H + ^{7}Li]$^+$, alongside *m/z* 504 and *m/z* 510, corresponding to [POPC – R$_1$COO]$^+$ and [POPC – R$_1$COO – H + ^{7}Li]$^+$ respectively.

25 **The influence of LiCl concentration on ion fragmentation.** Having observed that MALDI-MSMS of lithiated adducts enables the unambiguous identification of the lipid headgroup and both acyl chains, the range of lithium concentrations suitable for MALDI-MSMS analysis was investigated. For
30 POPE, the normalised intensities of the fragments corresponding to the headgroup ([OP(O)$_2$O(CH$_2$)$_2$NH$_3$ + H + ^{7}Li]$^+$), loss of the acyl chains from either the *sn*-1 or *sn*-2 position together with aminoethane ([POPE – R$_x$COO – (CH$_2$)$_2$NH$_3$ + H + ^{7}Li]$^+$) and the loss of the headgroup ([POPE
35 - OP(O)$_2$O(CH$_2$)$_2$NH$_3$]$^+$) were averaged for eight repeats at each of 6 concentrations of lithium chloride in the range 5 mM to 100 mM. No statistical differences were observed between the normalised intensities of the fragments at the different concentrations, regardless of whether the fragments
40 contained lithium or not, as shown in Fig. 4. Similar results were obtained for POPC, where the normalised intensities of the fragments corresponding to the headgroup ([OP(O)$_2$(CH$_2$)$_2$NMe$_3$+ 2H]$^+$), loss of the acyl chain from either the *sn*-1 or *sn*-2 position together with the
45 trimethylamine group ([POPC – R$_x$COO - NMe$_3$ – H + ^{7}Li]$^+$), loss of the acyl chains from either the *sn*-1 or *sn*-2 position

with and without lithium ([POPC – R$_x$COO]$^+$, [POPC – R$_x$COO – H + ^{7}Li]$^+$) and loss of the headgroup with and without lithium ([POPC - OP(O)$_2$(CH$_2$)$_2$NMe$_3$]$^+$ and [POPC -
50 OP(O)$_2$(CH$_2$)$_2$NMe$_3$ – H + ^{7}Li]$^+$), showed no statistical difference between the normalised fragment intensities over this concentration range (ESI, Fig. S4).
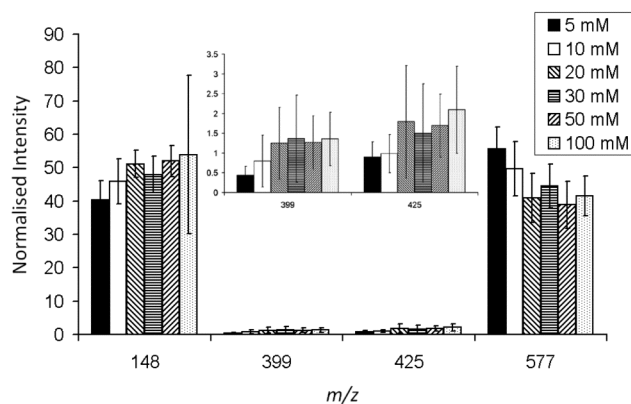

Fig. 4 Normalised intensities of [POPE + Li]$^+$ fragment peaks with
55 varying [LiCl] (5, 10, 20, 30, 50, 100 mM). The peaks with m/z 148, m/z 399, m/z 425 and m/z 577 refer to the fragments [OP(O)$_2$O(CH$_2$)$_2$NH$_3$ + Li + H]$^+$, [POPE - R$_2$COO – (CH$_2$)$_2$NH$_3$ + H + ^{7}Li]$^+$, [POPE - R$_1$COO – (CH$_2$)$_2$NH$_3$ + H + ^{7}Li]$^+$, and [POPE - OP(O)$_2$O(CH$_2$)$_2$NH$_3$]$^+$ respectively. Error bars represent 2× the standard deviation from 8 repeat scans in each
60 case.

Acyl chain identification by LIFT

Fragmentation of POPE ions. Successful identification of the acyl chain present at each position of a lipid requires that product ions can be identified in MSMS spectra that have
65 arisen by fragmentation processes at each of the *sn*-1 and *sn*-2 positions. Furthermore, in order for assignments to be unambiguous, there should be a difference in relative intensity that is statistically significant for the loss of equivalent fragments from each position. In order to examine whether
70 these criteria applied to fragmentation of POPE ions, twenty four MSMS spectra for each of [POPE + H]$^+$ and [POPE + Li]$^+$ were collected using an automated method to minimise experimental errors. Table 3 shows the different types of fragment observed which involve the neutral loss of fragments
75 from one or other of the acyl chains. For each of these types, the intensities of peaks corresponding to equivalent neutral losses from the *sn*-1 and *sn*-2 positions were normalised relative to each other. Two types of fragment from the parent [POPE + H]$^+$ were identified that showed a preferential loss of
80 a neutral acyl chain fragment from the *sn*-2 position (Fig. 5, Table 3, entries *a* and *b*). A further type of fragmentation of [POPE + Li]$^+$ involving the neutral loss of an acyl chain, [POPE – R$_x$COO – (CH$_2$)$_2$NH$_3$ + H + ^{7}Li]$^+$ was noted (Fig. 5, Table 3, entry *c*), although in this case the acyl chain fragment
85 was preferentially lost from the *sn*-1 position.

Three points can be made from these results. Firstly, as shown previously, the parent ions [POPE + H]$^+$ and [POPE + Li]$^+$ fragmented to give different product ions. Secondly, there were differences in the relative abundance of ions
90 corresponding to the neutral loss of acyl fragments from the *sn*-1 and *sn*-2 positions for the three different types of product ion (Table 3, a-c).
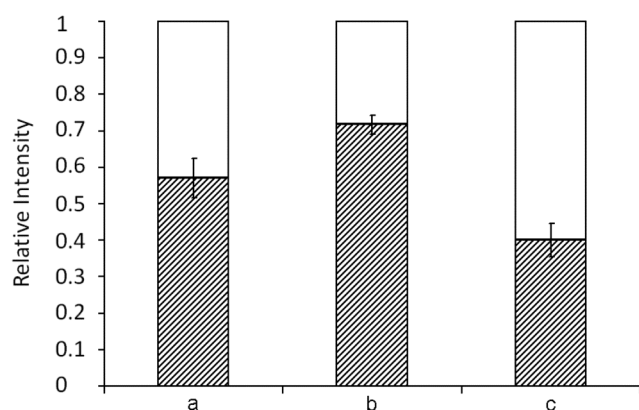
Fig. 5 The relative intensities of peaks corresponding to loss of the acyl chain from the *sn*-1 and *sn*-2 positions of different types of fragments of POPE from MSMS spectra of [POPE + H]$^+$ and [POPE + Li]$^+$. The white sections correspond to a loss from *sn*-1 position, shaded to the *sn*-2 position. Refer to Table 3 for identification of a-c. The error bars correspond to 2× the standard deviation of the data from 24 repeat scans.

Thirdly, the preference for neutral loss from the *sn*-2 over the *sn*-1 position for the protonated species was reversed for the lithiated species. Overall, the greatest difference in relative intensity corresponding to loss from *sn*-1 *vs* *sn*-2 was found for the [POPE – R$_x$CO + 2H]$^+$ fragmentation of [POPE + H]$^+$ (Table 3, entry b). The position of the acyl chains of POPE can therefore be identified from fragmentation in the presence or absence of lithium.

Table 3 Product ions corresponding to the loss of the acyl chain from the *sn*-1 or *sn*-2 positions of POPE observed in the MSMS spectra of [POPE + H]$^+$ and [POPE + Li]$^+$. The relative intensities of peaks corresponding to the loss of the acyl chains from the *sn*-1 and *sn*-2 positions have been normalised with respect to one another for each type of fragment.

	Parent Ion	Fragment[a]	RI, x = 1[b,c]	RI, x = 2[b,c]
a	[POPE + H]$^+$	[M – R$_x$COO]$^+$	0.43 ± 0.05	0.57 ± 0.05
b	[POPE + H]$^+$	[M – R$_x$CO + 2H]$^+$	0.28 ± 0.03	0.72 ± 0.03
c	[POPE + Li]$^+$	[M – R$_x$COO – (CH$_2$)$_2$NH$_3$ + H + ^{7}Li]$^+$	0.60 ± 0.05	0.40 ± 0.05

[a] x = 1 and x = 2 correspond to chains at the *sn*-1 and *sn*-2 positions of the lipid respectively.

[b] RI = relative intensity.

[c] The error is calculated as 2× the standard deviation of the data from 24 spectra.

Fragmentation of POPC ions. Twenty four MSMS spectra of [POPC + H]$^+$ and [POPC + Li]$^+$ were collected using an automated method and analysed in the same way as those of POPE. Similarly to POPE, the parent ions [POPC + H]$^+$ and [POPC + Li]$^+$ fragmented to give different product ions, and there were differences in the relative intensities of the peaks corresponding to loss of the acyl chains from the *sn*-1 *versus* the *sn*-2 positions for the different types of fragment (Table 4). More types of fragments of [POPC + H]$^+$ and [POPC + Li]$^+$ which involved the neutral loss of an acyl chain were observed than for POPE. However, in this case there were two types of fragment, one of the protonated parent and one of the lithium adduct, for which the intensities of the peaks corresponding to losses from the chains at the *sn*-1 and *sn*-2

positions were not significantly different (Fig. 6, Table 4, entries *a* and *d*), although in similar experiments with OPPC, formation of the equivalent product ions by loss of fragments from the *sn*-1 position was clearly favoured (Fig. S7 and Table S5, entries a and d).
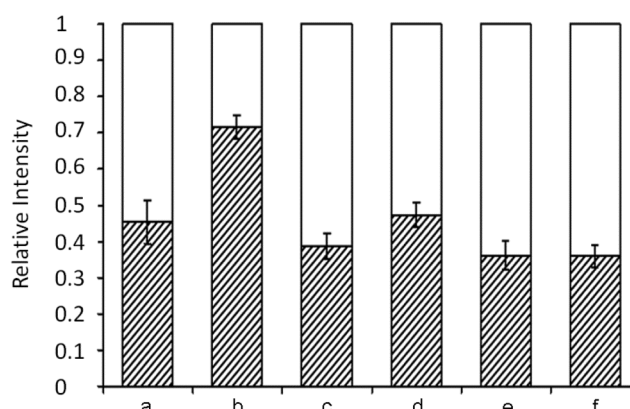

Fig. 6 The relative intensities of peaks corresponding to loss of the acyl chain from the *sn*-1 and *sn*-2 positions of different types of fragments of POPC from MSMS spectra of [POPC + H]$^+$ and [POPC + Li]$^+$. The white sections correspond to a loss from *sn*-1 position, shaded to the *sn*-2 position. Refer to Table 4 for identification of a-f. The error bars correspond to 2× the standard deviation of the data from 24 repeat scans.

For [POPC + H]$^+$, the [POPC – R$_x$CO + 2H]$^+$ fragment yielded peaks for which the ratio of the product ion intensities corresponding to generation of this fragment by loss from the *sn*-1 and the *sn*-2 positions lay outside a value of 0.5 : 0.5, within error, favouring loss from the *sn*-2 position (Fig. 6, Table 4, entry *b*).

Table 4 Product ions corresponding to the loss of the acyl chain from the *sn*-1 or *sn*-2 positions of POPC observed in the MSMS spectra of [POPC + H]$^+$ and [POPC + Li]$^+$. The relative intensities of peaks corresponding to the loss of the acyl chains from the *sn*-1 and *sn*-2 positions have been normalised with respect to one another for each type of fragmentation.

	Parent Ion	Fragment[a]	RI, x = 1[b,c]	RI, x = 2[b,c]
a	[POPC + H]$^+$	[M – R$_x$COO]$^+$	0.55 ± 0.06	0.45 ± 0.06
b	[POPC + H]$^+$	[M – R$_x$CO + 2H]$^+$	0.28 ± 0.03	0.72 ± 0.03
c	[POPC + Li]$^+$	[R$_x$CO]$^+$	0.61 ± 0.04	0.39 ± 0.04
d	[POPC + Li]$^+$	[M – R$_x$COO]$^+$	0.53 ± 0.03	0.47 ± 0.03
e	[POPC + Li]$^+$	[M – R$_x$COO – H + ^{7}Li]$^+$	0.64 ± 0.04	0.36 ± 0.04
f	[POPC + Li]$^+$	[M – R$_x$COO – NMe$_3$ – H + ^{7}Li]$^+$	0.64 ± 0.03	0.36 ± 0.03

[a] x = 1 and x = 2 correspond to chains at the *sn*-1 and *sn*-2 positions of the lipid respectively.

[b] RI = relative intensity.

[c] The error is calculated as 2× the standard deviation of the data from 24 spectra.

Three of the four types of fragment of [POPC + Li]$^+$ had a significant statistical difference between the normalised intensity of the peak corresponding to loss of the chain from the *sn*-1 position and the equivalent chain loss from the *sn*-2 position, namely [R$_x$CO]$^+$, [POPC – R$_x$COO – H + ^{7}Li]$^+$ and [POPC – R$_x$COO – NMe$_3$ – H + ^{7}Li]$^+$ (Fig. 6, Table 4, entries *c*, *e*, and *f* respectively).

Again, there was a difference in the acyl chain preferentially lost from each of the two parent ions, with a

greater peak intensity corresponding to the loss of the chain from the *sn*-2 position of the [POPC + H]$^+$ parent and a greater peak intensity corresponding to fragments involving a loss from the *sn*-1 position of [POPC + Li]$^+$. It was notable however, that in one case with OPPC, formation of the [R$_x$CO]$^+$ fragment occured preferentially through fragmentation at the *sn*-2 position (Fig. S7 and Table S5, entry c), in stark contrast to POPC. This would preclude using this fragment as a reliable means of determining the identity of the chains at each position.

Overall, the positions of the acyl chains can be determined from the product ion spectra of [POPC + H]$^+$ or [POPC + Li]$^+$, with the product ion spectrum of [POPC + Li]$^+$ providing more usable fragments (Table 4, entries e and f) and the product ions spectrum of [POPC + H]$^+$ providing the statistically most reliable fragment (Table 4, entry b).

Comparison of POPE and POPC ion fragmentation by LIFT.
A number of comparisons can be made between the results for POPE and POPC. The fragments of the protonated parents are the same, [M − R$_x$COO]$^+$ and [M − R$_x$CO + 2H]$^+$, and the relative intensities of the peaks corresponding to x = 1 and x = 2 are very similar for these fragments in both cases. Whilst there are more fragments of [POPC + Li]$^+$ than [POPE + Li]$^+$ that involve a loss of one or other of the acyl chains, there are nevertheless fragments, such as those involving loss of the headgroup ([POPE − R$_x$COO − (CH$_2$)$_2$NH$_3$ + H + ^{7}Li]$^+$ and [POPC − R$_x$COO − NMe$_3$ − H + ^{7}Li]$^+$), for which the relative intensities between the two lipids for x = 1 and x = 2 are similar. Where selective loss from the *sn*-1 or *sn*-2 chains was evident, it was notable that for both POPC and POPE, the protonated parents showed a preferential loss of the acyl chain from the *sn*-2 position, whilst the lithium adducts of both lipids preferentially lost the acyl chain from the *sn*-1 position. The finding that similar experiments with OPPC yield the reverse preference for the fragmentation position in one case demonstrates that the acyl chain plays a role in the formation of some fragments and obligates careful calibration of the instrument for each fragment type.

Comparison of LIFT and CID

Twenty five CID spectra of [POPC + H]$^+$ and [POPC + Li]$^+$ were collected, using an automated method to minimise experimental errors. Table 5 shows the different types of fragments observed which involve the loss of one or other of the acyl chains, along with the average percentage intensity of the peak corresponding to a loss from the *sn*-1 position relative to the peak corresponding to a loss from the *sn*-2 position for each fragment. Three main points can be identified from a comparison of the LIFT and CID data. Firstly, both fragmentation methods produce the same fragments involving the loss of one or other of the acyl chains, for both the protonated parent and the lithium adduct. Secondly, the relative intensities of x = 1 : x = 2 for the different fragments are the same between the LIFT data (Table 4) and the CID data (Table 5) in all but one case. For the fragments of [POPC + H]$^+$ the higher intensity of [POPC − R$_2$CO + 2H]$^+$ relative to [POPC − R$_1$CO + 2H]$^+$ was

particularly notable (ESI, Fig. S5 and Fig. S6). The only fragment of the [POPC + Li]$^+$ parent to show any difference from the LIFT data in terms of the relative intenities of loss from the *sn*-1 and *sn*-2 positions was the [M - R$_x$COO - NMe$_3$ – H + ^{7}Li]$^+$ peak. In this case, CID produced no difference in the peak intensities following loss from the *sn*-1 and *sn*-2 positions, contrasting the case for LIFT, where preferential loss from *sn*-1 occured. Thirdly, the CID data were less reproducible than the LIFT data, with larger standard deviations for all of the peak intensities.

Table 5 Product ions corresponding to the loss of the acyl chain from the *sn*-1 or *sn*-2 positions of POPC observed in CID spectra of [POPC + H]$^+$ and [POPC + Li]$^+$. The relative intensities of peaks corresponding to the loss of the acyl chains from the *sn*-1 and *sn*-2 positions have been normalised with respect to one another for each type of fragmentation.

Parent Ion	Fragment^a	RI, x = 1^{b,c}	RI, x = 2^{b,c}
[POPC + H]$^+$	[M − R$_x$COO]$^+$	0.45 ± 0.16	0.55 ± 0.16
[POPC + H]$^+$	[M − R$_x$CO + 2H]$^+$	0.29 ± 0.08	0.71 ± 0.08
[POPC + Li]$^+$	[R$_x$CO]$^+$	0.61 ± 0.11	0.39 ± 0.11
[POPC + Li]$^+$	[M − R$_x$COO]$^+$	0.53 ± 0.06	0.47 ± 0.06
[POPC + Li]$^+$	[M − R$_x$COO − H + ^{7}Li]$^+$	0.59 ± 0.08	0.41 ± 0.08
[POPC + Li]$^+$	[M - R$_x$COO - NMe$_3$ – H + ^{7}Li]$^+$	0.50 ± 0.08	0.50 ± 0.08

^{a} x = 1 and x = 2 correspond to chains at the *sn*-1 and *sn*-2 positions of the lipid respectively.

^{b} RI = relative intensity.

^{c} The error is calculated as 2× the standard deviation of the data from 25 spectra.

Conclusions

The objectives of this study were to examine the reproducibility of lipid fragmentation patterns in MSMS and determine the optimum conditions for complete characterisation of glycerophospholipids. Under the conditions employed, repeat MSMS analyses of POPE and POPC with and without the addition of lithium have shown that there is a statistical preference for the cleavage involving one acyl chain over the other for the generation of a number of different fragments, with opposite preferences for the protonated parent and the lithium adduct. This facilitated the unambiguous identification of POPC and POPE, including the identity of the headgroup and both acyl chains, and the positions of the acyl chains on the glycerol backbone of the lipid.

Three main advantages of analysis using LIFT in the presence of lithium were observed: i) more intense product ion peaks, facilitating lipid identification; ii) the frequent appearance of pairs of [M + H]$^+$ and [M + Li]$^+$ ions 6 mass units apart in both MS and product ion spectra that facilitate peak indentification; iii) the presence of a greater number of product ion peaks that enable lipid characterisation. However, the differences in fragmentation between POPC and OPPC indicate that each fragment type needs to be carefully assessed using appropriate standards. The most reliable peak for lipid identification in these experiments, both in terms of applicability to all of the lipids studied and the ratio of *sn*-1 to *sn*-2 fragmentation products, resulted by fragmentation of the protonated species. Fragmentation of POPC using CID was

shown to be less specific, although preferential cleavage was observed in some cases. The presence of more useful fragment peaks and the better reproducibility of peak intensities when using LIFT make this a better method for analysis of lipids than CID. Variations in the relative peak intensity following cleavage at the *sn*-1 and *sn*-2 positions, observed here for lithium adducts and elsewhere for sodium adducts,[5,16,20] highlight the need to rigorously validate each instrument for each method used for lipid analysis.

Notes and references

a Department of Chemistry, Centre for Bioactive Chemistry, University Science Laboratories, Durham, DH1 3LE, UK. Fax: +44 (0)191 3844737; Tel: +44 (0)191 3342107; E-mail: j.m.sanderson@durham.ac.uk; jackie.mosely@durham.ac.uk

b Department of Chemistry, University of Warwick, Coventry, CV4 7AL, UK.

1 A. Wieslander, S. Nordstrom, A. Dahlqvist, L. Rilfors and G. Lindblom, *Eur. J. Biochem.*, 1995, **227**, 734.
2 J. Schiller, R. Süβ, B. Fuchs, M. Müller, M. Petković, O. Zschörnig and H. Waschipy, *Eur. Biophys. J.*, 2007, **36**, 517.
3 G. Stubinger and O. Belgacem, *Anal. Chem.*, 2007, **79**, 3206.
4 M. Mank, B. Stahl and G. Boehm, *Anal. Chem.*, 2004, **76**, 2938.
5 K. A. Al-saad, W. F. Siems, H. H. Hill, V. Zabrouskov and N. R. Knowles, *J. Am. Soc. Mass Spectrom.*, 2003, **14**, 373.
6 S. N. Jackson, H.-Y. J. Wang and A. S. Woods, *J. Am. Soc. Mass Spectrom.*, 2007, **18**, 17.
7 X. Han and R. W. Gross, *J. Am. Soc. Mass Spectrom.*, 1995, **6**, 1202.
8 G. Stübiger, E. Pittenauer and G. Allmaier, *Anal. Chem.*, 2008, **80**, 1664.
9 S. Chen and K. W. Li, *J. Biochem.*, 1994, **116**, 811.
10 F. F. Hsu and J. Turk, *J. Am. Soc. Mass Spectrom.*, 2000, **11**, 892.
11 F. F. Hsu and J. Turk, *J. Mass Spectrom.*, 2000, **35**, 596.
12 F. F. Hsu and J. Turk, *J. Am. Soc. Mass Spectrom.*, 2003, **14**, 352.
13 F. F. Hsu, A. Bohrer and J. Turk, *J. Am. Soc. Mass Spectrom.*, 1998, **9**, 516.
14 H. Song, F. F. Hsu, J. Ladenson and J. Turk, *J. Am. Soc. Mass Spectrom.*, 2007, **18**, 1848.
15 S. N. Jackson, H.-Y. J. Wang and A. S. Woods, *J. Am. Soc. Mass Spectrom.*, 2005, **16**, 2052.
16 R. R. Landgraf, T. J. Garrett, N. A. Calcutt, P. W. Stacpoole and R. A. Yost, *Anal. Chem.*, 2007, **79**, 6862.
17 B. Fuchs, C. Schober, G. Richter, R. Süβ and J. Schiller, *J. Biochem. Biophys. Methods.*, 2007, **70**, 689
18 Z.-H. Huang, D. A. Gage and C. C. Sweeley, *J. Am. Soc. Mass Spectrom.*, 1992, **3**, 71.
19 J. L. Kerwin, A. R. Tuininga and L. H. Ericsson, *J. Lipid Res.*, 1994, **35**, 1102.
20 Y. H. Kim, J. S. Yoo and M. S. Kim, *Bull. Korean Chem. Soc.*, 1997, **18**, 874.
21 A. Kayganich and R. C. Murphy, *Anal. Chem.*, 1992, **64**, 2965.
22 S. Ramanadham, F. F. Hsu, S. Zhang, A. Bohrer, Z. Ma and J. Turk, *Biochim. Biophys. Acta*, 2000, **1484**, 251.
23 A. M. Hicks, C. J. DeLong, M. J. Thomas, M. Samuel and Z. Cui, *Biochim. Biophys. Acta*, 2006, **1761**, 1022
24 A. Hayashi, T. Matsubara, M. Morita, T. Kinoshita and T. J. Nakamura, *Biochemistry*, 1989, **106**, 264.
25 N. J. Jensen, K. B. Tomer and M. L. Gross, *Lipids*, 1986, **21**, 580.
26 D. Suckau, A. Resemann, M. Schuerenburg, P. Hufnagel, J. Franzen and A. Holle, *Anal. Bioanal. Chem.*, 2003, **367**, 952.
27 P. De Bievre and P.D.P. Taylor, *Int. J. Mass Spectrom. Ion Phys.*, 1993, **123**, 149.